






Gaia DR1 Evidence of Disrupting the Perseus Arm

Junichi Baba¹, Daisuke Kawata² , Noriyuki Matsunaga³, Robert J. J. Grand^{4,5} , and Jason A. S. Hunt⁶ ¹National Astronomical Observatory of Japan, Mitaka, Tokyo 181-8588, Japan²Mullard Space Science Laboratory, University College London, Holmbury St. Mary, Dorking, Surrey RH5 6NT, UK³Department of Astronomy, The University of Tokyo, 7-3-1 Hongo, Bunkyo-ku, Tokyo 113-0033, Japan⁴Heidelberger Institut für Theoretische Studien, Schloss-Wolfsbrunnengasse 35, D-69118 Heidelberg, Germany⁵Zentrum für Astronomie der Universität Heidelberg, Astronomisches Recheninstitut, Monchhofstr 12–14, D-69120 Heidelberg, Germany⁶Dunlap Institute for Astronomy and Astrophysics, University of Toronto, Toronto, ON M5S 3H4, Canada; jun.baba@nao.ac.jp, d.kawata@ucl.ac.uk

Received 2017 December 13; revised 2018 January 12; accepted 2018 January 15; published 2018 January 30

Abstract

We have discovered a clear sign of the disruption phase of the Perseus arm in the Milky Way using Cepheid variables, taking advantage of the accurately measured distances of Cepheids and the proper motions from *Gaia* Data Release 1. Both the Galactocentric radial and rotation velocities of 77 Cepheids within 1.5 kpc of the Perseus arm are correlated with their distances from the locus of the Perseus arm, as the trailing side is rotating faster and moving inward compared to the leading side. We also found a negative vertex deviation for the Cepheids on the trailing side, -27.6 ± 2.4 , in contrast to the positive vertex deviation in the solar neighborhood. This is, to our knowledge, the first direct evidence that the vertex deviation around the Perseus arm is affected by the spiral arm. We compared these observational trends with our *N*-body/hydrodynamics simulations based on a static density-wave spiral scenario and with those based on a transient dynamic spiral scenario. Although our comparisons are limited to qualitative trends, they strongly favor the conclusion that the Perseus arm is in the disruption phase of a transient arm.

Key words: astrometry – Galaxy: kinematics and dynamics – Galaxy: structure – methods: numerical

1. Introduction

How spiral arms in disk galaxies are created and maintained has been a long-standing question in galactic astronomy. For isolated disk galaxies there are two different theories of spiral arms that have different lifetimes (Dobbs & Baba 2014). The quasi-stationary density wave theory (hereafter SDW arm) characterizes spirals as rigidly rotating, long-lived wave patterns (i.e., $\gtrsim 1$ Gyr; Lin & Shu 1964; Bertin & Lin 1996). On the other hand, dynamic spiral theory (hereafter DYN arm) suggests spiral arms are differentially rotating, transient, recurrent patterns on a relatively short timescale, ~ 100 Myr (Sellwood & Carlberg 1984; Baba et al. 2009, 2013; Fujii et al. 2011; Grand et al. 2012a, 2012b; D’Onghia et al. 2013; Baba 2015).

Because a DYN arm is almost corotating with the stars at every radii, *N*-body simulation studies show that there should be a characteristic gas and stellar motion affected by the spiral arms (Grand et al. 2012b, 2016; Baba et al. 2013). Kawata et al. (2014) suggested that comparing the stellar velocity properties between the trailing and leading side of a spiral arm would provide crucial information regarding its origin (see also Hunt et al. 2015). The *Gaia* mission (Gaia Collaboration et al. 2016b) recently published its first data release (DR1; Gaia Collaboration et al. 2016a), including the proper motions and parallaxes for two million bright stars in common with the Tycho-2 catalog, known as the Tycho-*Gaia* astrometric solution (TGAS; Michalik et al. 2015; Lindegren et al. 2016). Hunt et al. (2017) reached a tentative conclusion favoring a DYN arm by finding a group of stars whose

Galactocentric rotation velocity is unexpectedly high owing to the torque from the Perseus arm. However, the feature was observed in stars in the solar neighborhood (distance < 0.6 kpc), which is still far away from the Perseus arm. Hence, it is difficult to conclude whether or not this feature is due to the Perseus arm.

Here, we investigate kinematics of Cepheid variables. They are bright variable stars and their distances are accurately measured thanks to their well-calibrated period–luminosity relation (Inno et al. 2013). Cepheids are also young stars whose ages are expected to be around 20–300 Myr (Bono et al. 2005). Such young stars are expected to have small velocity dispersion, and it is easier to find a systematic motion due to dynamical effects if it exists. Moreover, the age range of Cepheids is comparable to the lifetime of the DYN arm, and thus they are expected to be sensitive to the dynamical state of the spiral arms. Hence, Cepheids are a great tracer for testing the spiral arm scenario (see also Fernández et al. 2001; Griv et al. 2017). Thus, this letter uses Cepheids around the Perseus arm to study the dynamical state of the Perseus arm.

Section 2 describes our sample of Cepheids and shows their kinematic properties. Section 3 presents the results of comparisons between the observed Cepheids kinematics and what is seen in the simulations with different spiral models.

2. Peculiar Motions of Cepheids

We selected a sample of Cepheids in Genovali et al. (2014) where the distances were determined homogeneously by using near-infrared photometric data sets (also see Inno et al. 2013). Errors in distance modulus are estimated by Genovali et al. (2014) to be 0.05–0.07 mag for most of the Cepheids. We then cross-matched this sample with the TGAS catalog and with a sample of Cepheids whose radial velocity

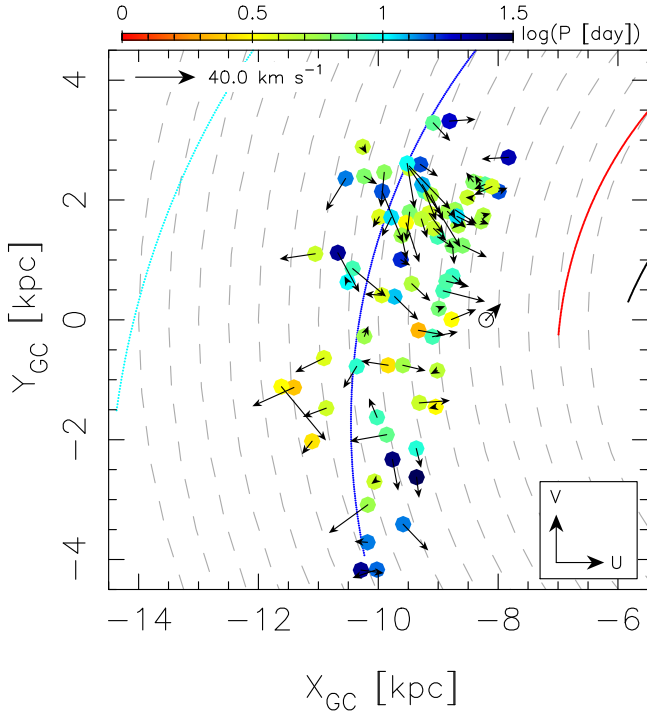


Figure 1. Face-on distribution of the selected Cepheids with arrows describing their peculiar velocities with color indicating their pulsation period ($\log P$). The cyan, blue, red, and black solid lines show the positions of the Outer, Perseus, Sagittarius, and Scutum spiral arms, respectively, measured in Reid et al. (2014). The open circle indicates the position of the Sun, and the arrow shows its peculiar motion.

are provided in Mel'nik et al. (2015) using TOPCAT (Taylor et al. 2005), giving a collection of 206 Cepheids with known locations and kinematics. We further limit the sample based on vertical position with respect to the Sun, $|z_{e,\max}| < 0.5$ kpc, where to take into account the error we define $z_{e,\max} = \sin(b)10^{(\mu_{\text{dm}} + \mu_{\text{dm},e} + 5.0)/5.0}/1000$ kpc, where b , μ_{dm} , and $\mu_{\text{dm},e}$ are the Galactic latitude, the distance modulus, and its error in magnitude, respectively. This limit was applied to eliminate clear outliers, although our sample shows a clear concentration around the Galactic plane, with more than 70% being located within 100 pc, as expected for young stars like Cepheids.

To eliminate the data with a large velocity or distance uncertainty, we discard the data whose uncertainty in velocity, $\sigma_V = \sqrt{\sigma_{V_{\text{lon}}}^2 + \sigma_{V_{\text{lat}}}^2 + \sigma_{V_{\text{HRV}}}^2}$, is larger than 20 km s^{-1} , where $\sigma_{V_{\text{lon}}}$, $\sigma_{V_{\text{lat}}}$, and $\sigma_{V_{\text{HRV}}}$ are the uncertainties of the velocity measurements in the direction of longitude, V_{lon} , latitude, V_{lat} , and heliocentric radial velocity, V_{HRV} . $\sigma_{V_{\text{lon}}}$ and $\sigma_{V_{\text{lat}}}$ are computed by taking the standard deviation of the Monte Carlo (MC) sampling of V_{lon} and V_{lat} , computed for randomly selected right ascension (R.A.) and declination (decl.) proper motions, using the 2D Gaussian probability distribution with their measured mean, standard error, and correlation between the R.A. and decl. proper motions, and distance from the Gaussian probability distribution of distance modulus with the mean of μ_{dm} and a standard deviation of $\mu_{\text{dm},e}$. These selections left 191 Cepheids in our sample.

From this sample, we choose Cepheids around the Perseus arm. We adopt the position of the Perseus arm locus as determined by Reid et al. (2014), which provides the distance and angle to the reference point from the Sun and the pitch

angle of the locus of the arm. We computed the mean distance, but projected on the Galactic plane, between the closest point of the locus of the Perseus arm and the Cepheids in our sample, d_{Per} , by MC sampling of the distance modulus for Cepheids and the distance between the Sun and the Galactic center of $R_0 = 8.2 \pm 0.1$ kpc (Bland-Hawthorn & Gerhard 2016).⁷ We selected Cepheids within $|d_{\text{Per}}| < 1.5$ kpc, which results in a final catalog of 77 Cepheids (see Figure 1).

We compute the Galactocentric radial velocity, U_{pec} , and rotation velocity, V_{pec} , after subtracting the circular velocity of the disk at the location of each Cepheid. Again, we used 10,000 MC samples to estimate the uncertainties of U_{pec} , V_{pec} , and d_{Per} , taking into account the mean and uncertainties of the distance modulus and proper motion for individual Cepheids and all the relevant Galactic parameters, such as $R_0 = 8.2 \pm 0.1$ kpc, the angular velocity of the Sun with respect to the Galactic center, $\Omega_{\odot} = 30.24 \pm 0.12 \text{ km s}^{-1} \text{ kpc}^{-1}$, the solar peculiar motion with respect to the Local Standard of the Rest (U_{\odot} , V_{\odot} , W_{\odot}) = $(10.0 \pm 1.0, 11.0 \pm 2.0, 7.0 \pm 0.5) \text{ km s}^{-1}$ (Bland-Hawthorn & Gerhard 2016), and the radial gradient of circular velocity, $dV_c/dR = -2.4 \pm 1.2 \text{ km s}^{-1} \text{ kpc}^{-1}$ (Feast & Whitelock 1997). We take the mean and standard deviation of U_{pec} , V_{pec} , and d_{Per} from the MC sample.

We first look at the correlation coefficients between U_{pec} and d_{Per} and between V_{pec} and d_{Per} . As shown in Figures 2(a) and (b), there is a significant positive correlation for both U_{pec} and V_{pec} against d_{Per} . We measure the correlations for each MC sampling described above and take the mean and dispersion of the measurements. Table 1 shows the correlation is statistically significant even after taking into account the observational errors and uncertainties of the Galactic parameters. The correlation is stronger in V_{pec} than U_{pec} .

Following the idea of Kawata et al. (2014), we compared the velocity distribution of 47 Cepheids on the trailing side (defined as $0.2 < d_{\text{Per}} < 1.5$ kpc) and that of 16 Cepheids on the leading side ($-1.5 < d_{\text{Per}} < -0.2$ kpc) of the Perseus arm.⁸ We found a significant offset in the mean velocity of these samples as expected from the correlation with d_{Per} (see also Table 1). The mean velocity in both $\langle U_{\text{pec}} \rangle$ and $\langle V_{\text{pec}} \rangle$ is higher on the trailing side. To our knowledge, these results are the first statistically significant observational evidence of the difference in dynamical properties of stars on different sides of the spiral arm.

Furthermore, we calculated the vertex deviation, $l_v = 0.5 \times \arctan(2\sigma_{UV}^2/(\sigma_U^2 - \sigma_V^2))$ (including the correction term suggested by Vorobyov & Theis 2008, for the case of $\sigma_V > \sigma_U$), where σ_{UV}^2 is the covariance between U_{pec} and V_{pec} , for the sample on the trailing and leading sides (see their $U_{\text{pec}}-V_{\text{pec}}$ distribution in Figures 2(c) and (d)). The results are summarized in Table 1. On the leading side, the number of Cepheids in the sample is too small to measure l_v confidently. On the trailing side, in contrast, the vertex deviation is clearly negative, which is opposite to the positive one (about $+20^\circ$) of the young stars in the local solar neighborhood (e.g., Dehnen & Binney 1998; Rocha-Pinto et al. 2004). To our knowledge, this is the first detection of the change of sign of the vertex

⁷ In our MC sampling, for simplicity, we fixed the pitch angle, but only changed the Galactocentric radius of the reference point of the Perseus arm for a sampled R_0 , although the pitch angle also depends on R_0 .

⁸ We excluded Cepheids within $|d_{\text{Per}}| < 0.2$ kpc considering the uncertainty of the locus of the Perseus arm.

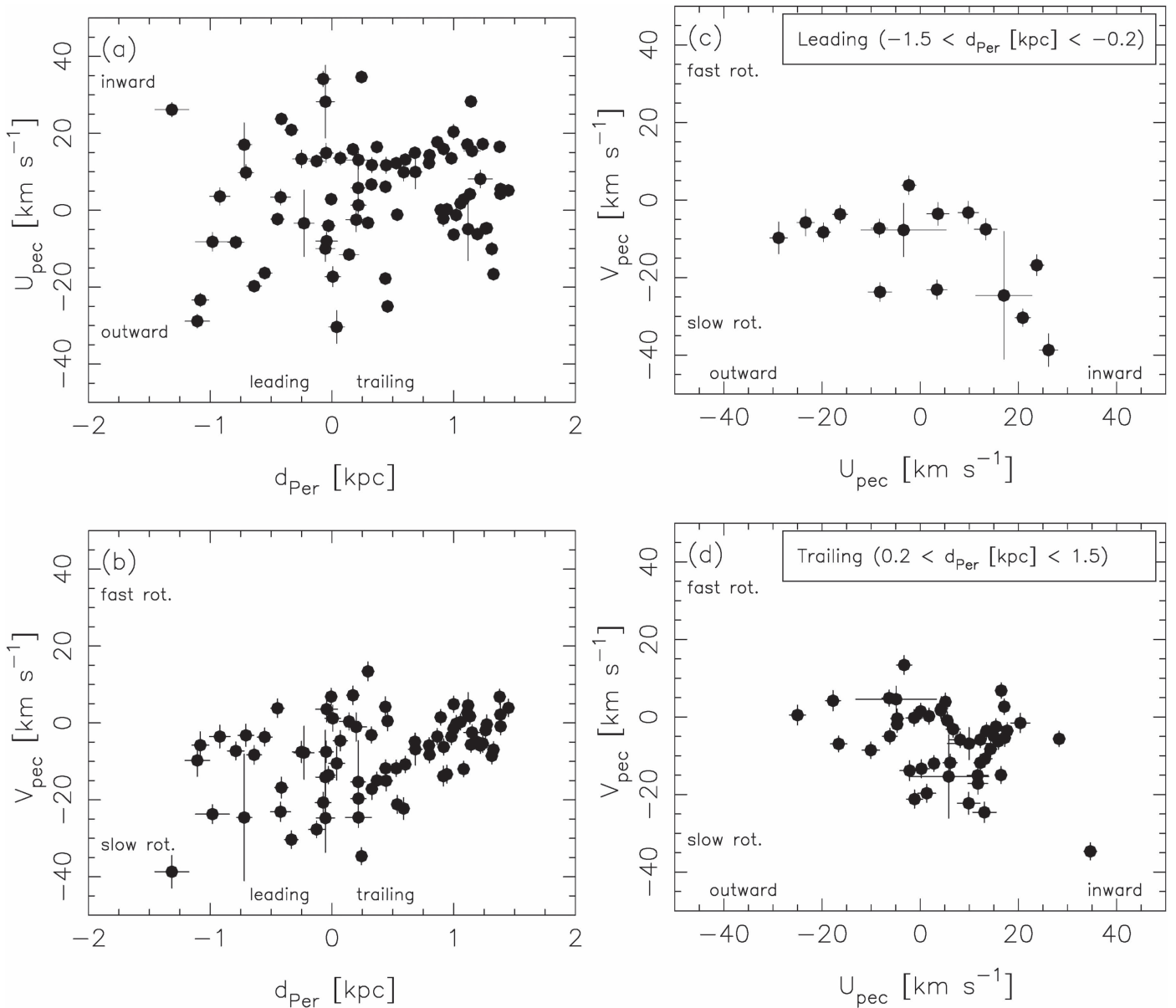


Figure 2. (a) $U_{\text{pec}}-d_{\text{Per}}$ and (b) $V_{\text{pec}}-d_{\text{Per}}$ distributions of our Cepheid sample. Note that U_{pec} is positive in the direction toward the Galactic center, and V_{pec} is positive in the direction of the Galactic rotation. ((c) and (d)) $U_{\text{pec}}-V_{\text{pec}}$ distributions of our Cepheid sample in leading and trailing sides of the Perseus arm, respectively.

deviation near the spiral arms. Such a change is expected in various spiral arm models (Roca-Fàbrega et al. 2014).

Finally, we discuss the effect of interstellar reddening and extinction considering its importance for the objects in the disk (Matsunaga 2017). Inno et al. (2013) assumed the total-to-selective reddening ratio of Cardelli et al. (1989), which is different from some of the recent values (e.g., Nishiyama et al. 2006; Alonso-García et al. 2017). The reddenings of the Cepheids around the Perseus arm are, however, relatively small, $E_{J-K_s} \leq 0.5$ mag, and the uncertainty caused by the extinction law (up to 7% in distance) does not change our results.

3. Dynamic Nature of the Perseus Arm

We compare our findings with N -body/hydrodynamic simulations with different spiral models. The simulations

include self-gravity, radiative cooling, star formation, and stellar feedback (Saitoh et al. 2008; Saitoh & Makino 2009). The DYN arm model is a barred spiral galaxy formed from an initial axisymmetric model, spontaneously. The bar is an almost stable pattern, but the amplitudes, pitch angles, and rotational frequencies of the spiral arms change within a few hundred million years (Baba 2015). The SDW models are from Baba et al. (2016) and have a rigidly rotating two-armed spiral (external potential) with a pitch angle of 12° and a spiral amplitude of 3%. To study the impact of the location of the corotation radius (R_{cr}), we used two SDW models with $R_{\text{cr}} = 8$ kpc (e.g., Fernández et al. 2001) and 16 kpc (e.g., Lin et al. 1969).

To compare the simulations with the observational data, we have applied the same analysis as Section 2 for the simulations. First, we identify a spiral arm similar to the

Table 1
Kinematics of Cepheids and Model Results

	Cepheids (number)	SDW ($R_{\text{cr}} = 8$)	SDW ($R_{\text{cr}} = 16$)	DYN ($t = 2.59$)	DYN ($t = 2.62$)
$U_{\text{pec}}-d_{\text{Per}}$ Corr.	0.14 ± 0.02 (77)	0.21 ± 0.07	-0.80 ± 0.02	-0.21 ± 0.03	0.14 ± 0.03
$V_{\text{pec}}-d_{\text{Per}}$ Corr.	0.40 ± 0.03 (77)	-0.34 ± 0.03	-0.47 ± 0.03	0.062 ± 0.04	0.15 ± 0.03
Trailing Side ($0.2 < d_{\text{Per}} < 1.5$ kpc)					
$\langle U_{\text{pec}} \rangle$ (km s $^{-1}$)	6.1 ± 1.0 (47)	-7.0 ± 0.5	-24.3 ± 1.8	-11.4 ± 0.9	4.6 ± 0.8
$\langle V_{\text{pec}} \rangle$ (km s $^{-1}$)	-6.3 ± 2.0 (47)	-8.5 ± 0.4	-8.5 ± 0.7	-7.5 ± 0.8	-3.8 ± 0.8
l_v (deg)	-27.6 ± 2.4 (47)	-11.5 ± 5.6	3.1 ± 5.1	27.4 ± 5.8	-42.4 ± 5.2
Leading Side ($-1.5 < d_{\text{Per}} < -0.2$ kpc)					
$\langle U_{\text{pec}} \rangle$ (km s $^{-1}$)	0.49 ± 1.2 (16)	-10.4 ± 2.9	21.5 ± 0.7	-1.1 ± 1.5	-3.0 ± 1.4
$\langle V_{\text{pec}} \rangle$ (km s $^{-1}$)	-13.4 ± 2.0 (16)	-1.7 ± 1.1	0.46 ± 0.54	-11.2 ± 1.0	-11.9 ± 0.9
l_v (deg)	-28.2 ± 6.5 (16)	9.0 ± 3.3	-1.2 ± 10.9	20.8 ± 2.9	22.5 ± 1.9

Perseus arm in terms of the Galactocentric radial range. Then, we selected young star particles (50–200 Myr) around the arm that are located in a radial and azimuthal range similar to that of our Cepheids sample. Note that the pitch angle of our SDW models is not tuned to match the Perseus arm, but is the one to best explain both the Scutum and Perseus arms with a single pitch angle. Also, the pitch angle of the DYN model is changing as time goes on. Thus, for both SDW and DYN models we measure the distance of the particles from the gas arm (to be consistent with the identification of the arm by the star-forming regions in Reid et al. 2014), d_{arm} , irrespective of the pitch angles of the spiral arms, and consider it the same as d_{Per} for our Cepheids data analysis. The results of the simulations are summarized in Table 1 and are shown in Figure 3.

We first compare the observation with the SDW models. As shown on left side of the panels of Figure 3, SDW ($R_{\text{cr}} = 16$) reproduces none of the observed trend, suggesting that this model is clearly rejected. On the other hand, SDW ($R_{\text{cr}} = 8$) shows some degree of success in the positive correlation coefficient of $U_{\text{pec}}-d_{\text{Per}}$ (Figure 3(a)) and a negative vertex deviation in the trailing side (Figure 3(d)). However, this model fails to reproduce the positive correlation in $V_{\text{pec}}-d_{\text{Per}}$ (Figure 3(a)). Hence, we conclude that irrespective of R_{cr} (i.e., the pattern speed), it is difficult for the SDW models to explain the observed features in Section 2. This does not mean that we can reject the SDW scenario. Indeed, we have not explored models of different pitch angles and/or different strength of the arms; moreover, our SDW models do not include the bar, which is likely to affect the dynamical features (e.g., Monari et al. 2016). Although these different kinds of models need to be tested against our observed Cepheid kinematics, the SDW spiral models tend to show a regular trend in stellar kinematics around the spiral arms (e.g., Roca-Fàbrega et al. 2014; Antoja et al. 2016; Pasetto et al. 2016). We therefore expect that the positive correlation of $V_{\text{pec}} - d_{\text{Per}}$ is difficult to obtain in the SDW model alone.

We then compare the DYN model with the observations. The right side of the panels of Figure 3 shows the results around a spiral arm that grew and were disrupted around $t = 2.59$ and $t = 2.62$ Gyr (indicated with vertical dotted-dashed lines), respectively. As shown in Baba et al. (2013) and Grand et al. (2014), the kinematic properties of the stars around the DYN spiral arms change with time. As a result, the growing

phase of the DYN arm (at $t \sim 2.59$ Gyr) is not consistent with the observed properties.

Among our models, the disruption phase (at $t \sim 2.62$ Gyr) of the DYN arm is qualitatively the best at reproducing the observed trends. The correlation coefficients between velocity are both positive, as observed, although the correlation is stronger for $V_{\text{pec}}-d_{\text{Per}}$ in the observational data (Figure 3(a)). As shown in Figures 3(b) and (c), both $\langle U_{\text{pec}} \rangle$ and $\langle V_{\text{pec}} \rangle$ are also in good agreement with our observational results, and the trailing side shows higher values than the leading side. The observed negative vertex deviation is also reproduced in the trailing side. On the other hand, the leading side shows less sensitivity of vertex deviation to the phase of the DYN arm, i.e., always positive, which is inconsistent with our observed trend (Figure 3(d)). However, the measurement of vertex deviation in the leading side is less reliable. Hence, the disruption phase of the DYN arm shows qualitative agreement with the high-confidence results of our Cepheid data. Considering that our N -body simulations are still far from the real Milky Way because of lack of physical processes and lack of observational constraints, it is striking to find this level of agreement between the disruption phase of our simulated DYN arm and the observed trends found in our Cepheid data. We therefore conclude that the disruption phase of a DYN spiral arm like that seen in our simulation is the most likely scenario for the Perseus arm in the Milky Way.

It is known that the age of Cepheids is well correlated with their pulsation period ($\log P$; e.g., Bono et al. 2005). We color coded Cepheids by $\log P$ in Figure 1. We found no clear correlation between the age of Cepheids with the position with respect to the arm. The SDW scenario predicts a clear correlation between the age of stars and the distance from the arm (e.g., Dobbs & Pringle 2010). Hence, this is also against the prediction from the SDW scenario, but it is more consistent with the DYN arm scenario (e.g., Grand et al. 2012a).

Interestingly, according to Reid et al. (2014), the pitch angle of the Perseus arm (9.4 ± 1.4) is smaller than the Scutum arm (19.8 ± 2.6), which is the other major arm. N -body simulations of DYN arms predict that the pitch angle of spiral arms in the disruption phase would be smaller, because the arms are winding and disrupting (Baba et al. 2013; Grand et al. 2013). Therefore, if the Perseus arm does indeed have a small pitch angle, it is also consistent with the arm being in the disruption phase. We will further test the disruption phase scenario of the Perseus arm with future *Gaia* data releases.

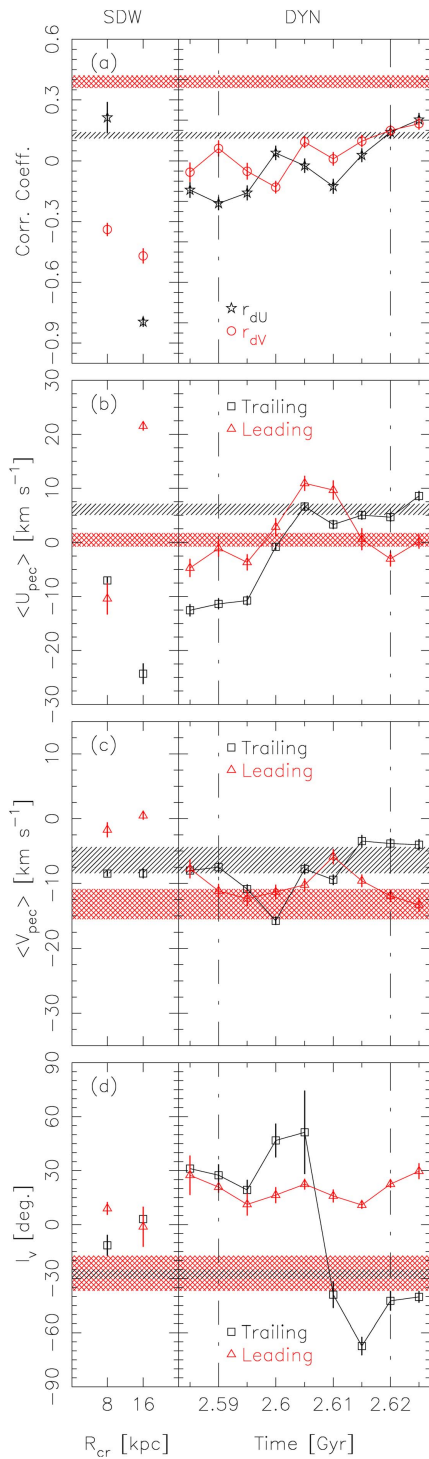


Figure 3. Comparison between the models and the observed kinematics of Cepheids in terms of correlations of $U_{pec}-d_{Per}$ and $V_{pec}-d_{Per}$ (a), mean U_{pec} (b), mean V_{pec} (c), and the vertex deviation, l_v (d). Horizontal shaded areas in black and red indicate the observed values and the 1σ uncertainty ranges for the $U_{pec}-d_{Per}$ and $V_{pec}-d_{Per}$ correlations, respectively, in the top panel, while the measured values in the trailing (leading) side of the arm are indicated by different colors in the other panels. The model results are shown as open symbols with error bars. Black stars (red circles) in the top panel show the $U_{pec}-d_{Per}$ ($V_{pec}-d_{Per}$) correlation. In the second, third, and bottom panels, black squares (red triangles) show the measured values in the trailing (leading) side of the arm. Note that the left side of the panels shows the SDW model results for two different R_{cr} values, whereas on the right side the DYN model results are presented as a function of time. These results are also summarized in Table 1.

We are grateful to the referee for useful suggestions that helped improve this Letter. We also thank Nobuyuki Sakai for useful advice on analysis of astrometric data. We thank Jo Bovy for making `galpy` (Bovy 2015), which is used for coordinate transformation, publicly available. JB was supported by the Japan Society for the Promotion of Science (JSPS) Grant-in-Aid for Young Scientists (B) grant number 26800099. DK acknowledges the support of the UK’s Science & Technology Facilities Council (STFC grant ST/N000811/1). NM is grateful to Grant-in-Aid (KAKENHI, No. 26287028) from the Japan Society for the Promotion of Science (JSPS). JASH is supported by a Dunlap Fellowship at the Dunlap Institute for Astronomy & Astrophysics, funded through an endowment established by the Dunlap family and the University of Toronto. RG acknowledges support by the DFG Research Centre SFB-881 “The Milky Way System” through project A1. This work has made use of data from the European Space Agency (ESA) mission *Gaia* (<https://www.cosmos.esa.int/gaia>), processed by the *Gaia* Data Processing and Analysis Consortium (DPAC, <https://www.cosmos.esa.int/web/gaia/dpac/consortium>). Funding for the DPAC has been provided by national institutions, in particular the institutions participating in the *Gaia* Multilateral Agreement. The simulations reported in this paper were carried out on facilities of Center for Computational Astrophysics (CfCA), National Astronomical Observatory of Japan.

ORCID iDs

Daisuke Kawata <https://orcid.org/0000-0001-8993-101X>
 Robert J. J. Grand <https://orcid.org/0000-0001-9667-1340>
 Jason A. S. Hunt <https://orcid.org/0000-0001-8917-1532>

References

- Alonso-García, J., Minniti, D., Catelan, M., et al. 2017, *ApJL*, **849**, L13
 Antoja, T., Roca-Fàbrega, S., de Bruijne, J., & Prusti, T. 2016, *A&A*, **589**, A13
 Baba, J. 2015, *MNRAS*, **454**, 2954
 Baba, J., Asaki, Y., Makino, J., et al. 2009, *ApJ*, **706**, 471
 Baba, J., Morokuma-Matsui, K., Miyamoto, Y., Egusa, F., & Kuno, N. 2016, *MNRAS*, **460**, 2472
 Baba, J., Saitoh, T. R., & Wada, K. 2013, *ApJ*, **763**, 46
 Bertin, G., & Lin, C. C. (ed.) 1996, *Spiral Structure in Galaxies a Density Wave Theory* (Cambridge, MA: MIT Press)
 Bland-Hawthorn, J., & Gerhard, O. 2016, *ARA&A*, **54**, 529
 Bono, G., Marconi, M., Cassisi, S., et al. 2005, *ApJ*, **621**, 966
 Bovy, J. 2015, *ApJS*, **216**, 29
 Cardelli, J. A., Clayton, G. C., & Mathis, J. S. 1989, *ApJ*, **345**, 245
 Dehnen, W., & Binney, J. J. 1998, *MNRAS*, **298**, 387
 Dobbs, C., & Baba, J. 2014, *PASA*, **31**, 35
 Dobbs, C. L., & Pringle, J. E. 2010, *MNRAS*, **409**, 396
 D’Onghia, E., Vogelsberger, M., & Hernquist, L. 2013, *ApJ*, **766**, 34
 Feast, M., & Whitelock, P. 1997, *MNRAS*, **291**, 683
 Fernández, D., Figueras, F., & Torra, J. 2001, *A&A*, **372**, 833
 Fujii, M. S., Baba, J., Saitoh, T. R., et al. 2011, *ApJ*, **730**, 109
 Gaia Collaboration, et al. 2016a, *A&A*, **595**, A2
 Gaia Collaboration, et al. 2016b, *A&A*, **595**, A1
 Genovali, K., Lamasle, B., Bono, G., et al. 2014, *A&A*, **566**, A37
 Grand, R. J. J., Kawata, D., & Cropper, M. 2012a, *MNRAS*, **426**, 167
 Grand, R. J. J., Kawata, D., & Cropper, M. 2012b, *MNRAS*, **421**, 1529
 Grand, R. J. J., Kawata, D., & Cropper, M. 2013, *A&A*, **553**, A77
 Grand, R. J. J., Kawata, D., & Cropper, M. 2014, *MNRAS*, **439**, 623
 Grand, R. J. J., Springel, V., Kawata, D., et al. 2016, *MNRAS*, **460**, L94
 Griv, E., Hou, L.-G., Jiang, I.-G., & Ngeow, C.-C. 2017, *MNRAS*, **464**, 4495
 Hunt, J. A. S., Kawata, D., Grand, R. J. J., et al. 2015, *MNRAS*, **450**, 2132
 Hunt, J. A. S., Kawata, D., Monari, G., et al. 2017, *MNRAS*, **467**, L21
 Inno, L., Matsunaga, N., Bono, G., et al. 2013, *ApJ*, **764**, 84
 Kawata, D., Hunt, J. A. S., Grand, R. J. J., Pasetto, S., & Cropper, M. 2014, *MNRAS*, **443**, 2757

- Lin, C. C., & Shu, F. H. 1964, [ApJ](#), **140**, 646
- Lin, C. C., Yuan, C., & Shu, F. H. 1969, [ApJ](#), **155**, 721
- Lindgren, L., Lammers, U., Bastian, U., et al. 2016, [A&A](#), **595**, A4
- Matsunaga, N. 2017, [EPJWC](#), **152**, 01007
- Mel'nik, A. M., Rautiainen, P., Berdnikov, L. N., Dambis, A. K., & Rastorguev, A. S. 2015, [AN](#), **336**, 70
- Michalik, D., Lindgren, L., & Hobbs, D. 2015, [A&A](#), **574**, A115
- Monari, G., Famaey, B., Siebert, A., et al. 2016, [MNRAS](#), **461**, 3835
- Nishiyama, S., Nagata, T., Kusakabe, N., et al. 2006, [ApJ](#), **638**, 839
- Pasetto, S., Natale, G., Kawata, D., et al. 2016, [MNRAS](#), **461**, 2383
- Reid, M. J., Menten, K. M., Brunthaler, A., et al. 2014, [ApJ](#), **783**, 130
- Roca-Fàbrega, S., Antoja, T., Figueras, F., et al. 2014, [MNRAS](#), **440**, 1950
- Rocha-Pinto, H. J., Flynn, C., Scalo, J., et al. 2004, [A&A](#), **423**, 517
- Saitoh, T. R., Daisaka, H., Kokubo, E., et al. 2008, [PASJ](#), **60**, 667
- Saitoh, T. R., & Makino, J. 2009, [ApJL](#), **697**, L99
- Sellwood, J. A., & Carlberg, R. G. 1984, [ApJ](#), **282**, 61
- Taylor, M. B. 2005, in ASP Conf. Ser. 347, *Astronomical Data Analysis Software and Systems XIV*, ed. P. Shopbell, M. Britton, & R. Ebert (San Francisco, CA: ASP), 29
- Vorobyov, E. I., & Theis, C. 2008, [MNRAS](#), **383**, 817